Annealing-Free High-Mobility Diketopyrrolopyrrole–Quaterthiophene Copolymer for Solution-Processed Organic Thin Film Transistors

Yuning Li,[†,‡,*] Prashant Sonar,[†] Samarendra P. Singh,[†] Mui Siang Soh,[†] Martin van Meurs,[§] and Jozel Tan[§]

[†]Institute of Materials Research and Engineering (IMRE), Agency for Science, Technology, and Research (A*STAR), 3 Research Link, Singapore 117602

[‡]Department of Chemical Engineering and Waterloo Institute for Nanotechnology (WIN), University of Waterloo, 200 University Avenue West, Waterloo, Ontario, Canada N2L 3G1

[§]Institute of Chemical and Engineering Sciences, A*STAR, 1 Pesek Road, Jurong Island, Singapore 627833

S *Supporting Information*

ABSTRACT: A donor–acceptor polymer semiconductor, PDQT, comprising diketopyrrolopyrrole (DPP) and β-unsubstituted quaterthiophene (QT) for organic thin film transistors (OTFTs) is reported. This polymer forms ordered layer-by-layer lamellar packing with an edge-on orientation in thin films even without thermal annealing. The strong intermolecular interactions arising from the fused aromatic DPP moiety and the DPP–QT donor–acceptor interaction facilitate the spontaneous self-assembly of the polymer chains into close proximity and form a large $\pi-\pi$ overlap, which are favorable for intermolecular charge hopping. The well-interconnected crystalline grains form efficient intergranular charge transport pathways. The desirable chemical, electronic, and morphological structures of PDQT bring about high hole mobility of up to 0.97 cm^2/(V·s) in OTFTs with polymer thin films annealed at a mild temperature of 100 °C and similarly high mobility of 0.89 cm^2/(V·s) for polymer thin films even without thermal annealing.
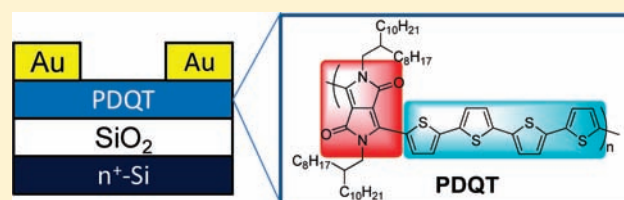
INTRODUCTION

Printed organic thin film transistors (OTFTs) are of extensive research interest mainly because they can be fabricated at low costs by using printing techniques.[1] In comparison to small molecular or oligomeric materials, polymer semiconductors have superior solution processability and mechanical robustness. However, solution-processed polymer thin films always comprise amorphous regions along with crystalline domains, which is the primarily reason for their relatively poor charge carrier transport properties.[1a,1c] Thermal annealing at around 150 °C or higher is a commonly used practice to improve the molecular organization of the polymer thin films to obtain higher charge carrier mobility. Although high field effect mobility of up to ~0.6 cm^2/(V·s) has been achieved for certain polymers[2,3] with the aid of thermal annealing, the mobility for nonannealed polymer thin films is in general significantly lower. The thermal annealing step is time-consuming and usually needs to be conducted under vacuum or in an inert atmosphere to prevent the polymer thin films from adverse oxidative degradation. This poses a challenge in the cost-effective production of printed OTFTs in a high-throughput, roll-to-roll manufacturing manner. Another potential issue associated with high-temperature thermal annealing is that common plastic substrates such as poly(ethylene terephthalate) (PET) films become dimensionally unstable at a temperature of 150 °C

or higher.[4] To eliminate the thermal annealing step, we previously designed a polymer, poly(4,8-dihexyl-2,6-bis(3-hexylthiophen-2-yl)benzo[1,2-b:4,5-b′]dithiophene) (PBTBDT), which comprises a fused aromatic ring structure, benzo[1,2-b:4,5-b′]-dithiophene (BDT).[5] Incorporation of BDT in this polymer facilitated the self-assembly of the polymer chains into a highly ordered crystalline structure through strong $\pi-\pi$ interactions exerted by the fused BDT units. In addition, the side chain substitution of PBTBDT was engineered with adequately populated straight alkyl groups to avoid the interchain interdigitation, which allowed the desirable polymer main chain packing to take place preferentially. As a result, PBTBDT could readily form molecularly orientated thin films comprising large crystal grains (up to a few micrometers) after solution deposition without thermal annealing. High mobility of ~0.25 cm^2/(V·s) was achieved for nonannealed PBTBDT thin films in OTFTs.[5] In this study, we utilize the intermolecular donor–acceptor interaction as an additional driving force to assist the self-assembly of the polymer main chains from solution to thin films. Furthermore, long, branched alkyl side chains are used to improve the solubility of the resulting polymer as well as prevent the interference of the

Chart 1. Structures of Thieno[3,2-b]thiophene (X = S; Y = CH), Thiazolo[3,2-b]thiazole (X = S; Y = N), Selenopheno[3,2-b]selenophene (X = Se; Y = CH), Diketopyrrolopyrrole (DPP), PDBT-co-TT, and DPP−Oligothiophene Copolymers (m ≥ 0)[a]

5-5-membered fused ring
X = S or Se
Y = CH or N

PDBT-co-TT

DPP

DPP-oligothiophene copolymer
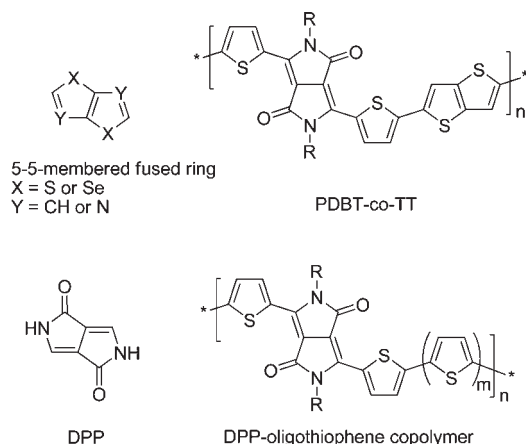
[a] R is a substituent such as an alkyl.

side chain crystallization with the desirable main chain packing. Specifically, we have chosen 2,5-dihydropyrrolo[3,4-c]pyrrole-1,4-dione or diketopyrrolopyrrole (DPP) as an electron acceptor and β-unsubstituted quaterthiophene (QT) as an electron donor to form a PDQT copolymer (m = 2 in Chart 1). This polymer can spontaneously form crystalline thin films with an edge-on molecular orientation after solution deposition without a subsequent high-temperature annealing step. High hole mobility of up to 0.97 cm^2/(V·s) was achieved for OTFTs using PDQT thin films annealed at a mild temperature of 100 °C. Similarly high mobility of 0.89 cm^2/(V·s) was obtained for devices with nonannealed polymer thin films.

■ RESULTS AND DISCUSSION

Among condensed aromatic structures, five−five-membered fused heterocyclic aromatics such as thieno[3,2-b]thiophene,[2,6] thiazolo[5,4-d]thiazole,[7] and selenopheno[3,2-b]selenophene[8] are useful building blocks for p-type polymer semiconductors for OTFTs (Chart 1). Another analogous fused aromatic framework, DPP (Chart 1), has also been found a good moiety for constructing polymers for OTFT applications.[9] Very recently, we reported that the combination of the thieno[3,2-b]thiophene unit as a donor and the DPP unit as an acceptor led to a donor−acceptor copolymer, PDBT-co-TT (Chart 1), which showed high hole mobility of up to 0.94 cm^2/(V·s).[10] The enhanced intermolecular interactions due to the donor−acceptor interaction are thought responsible for the observed high charge carrier transport performance. However, PDBT-co-TT thin films require annealing at a high temperature of 200 °C to maximize the mobility likely due to the rigid condensed thieno[3,2-b]thiophene moiety. In this study we use the unsubstituted bithiophene (m = 2, Chart 1), instead of thieno[3,2-b]thiophene, to slightly weaken the main chain interactions to enhance the molecular ordering capability of the resulting polymer PDQT at lower temperatures. Previously, DPP−bithiophene and DPP−terthiophene copolymers (m = 0 and 1 in Chart 1) have been reported, which showed hole mobility of less than ∼0.1 cm^2/(V·s) in OTFTs.[9c−9e] Due to the strong electron-accepting nature of
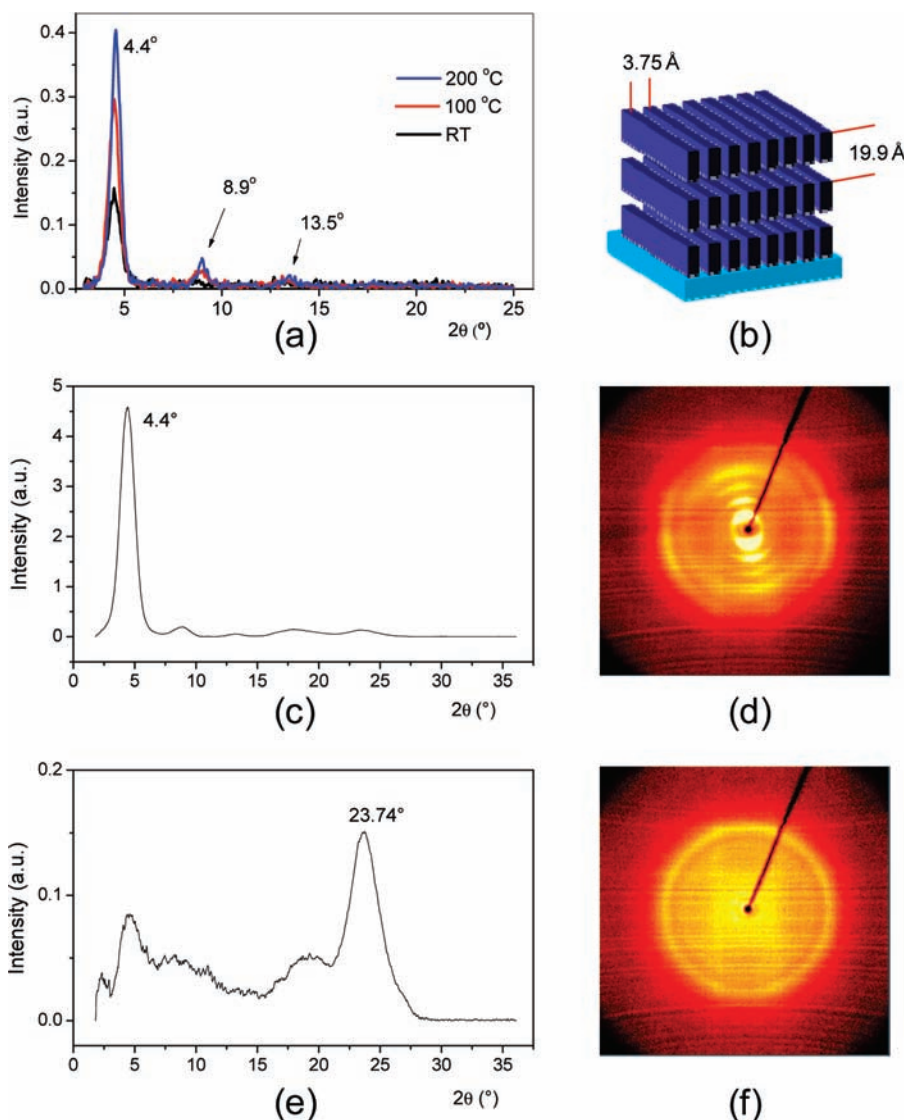
DPP, these polymers showed ambipolar transport characteristics, i.e., capable of conducting both holes and electrons in OTFTs.[9d,9e] Here, the use of a longer oligothiophene, β-unsubstituted QT, in PDQT is expected to adequately compensate for the excessive electron-accepting effect of DPP to enhance the hole transport characteristics.

The synthetic route to PDQT is outlined in Scheme 1. Compounds **1**, **2**, and **3** were prepared in moderate to good isolated yields according to the established methods.[10] Stille coupling polymerization of **3** with 5,5′-bis(trimethylstannyl)-bithiophene in the presence of a catalytic amount of Pd-(PPh$_3$)$_2$Cl$_2$ in toluene at 90 °C for 48 h afforded polymer PDQT. The polymer was purified by using Soxhlet extraction with acetone, methanol, and hexane successively to remove the low molecular mass fractions and other impurities. The final polymer was obtained in a nearly quantitative yield (∼99%). PDQT is readily soluble in tetrahydrofuran (THF), toluene, chloroform, chlorobenzene, and a number of other organic solvents. The molecular weights of PDQT were determined by gel permeation chromatography (GPC) against polystyrene standards. It was found that the molecular weights (number average molecular weight (M_n) of 106 000; weight average molecular weight (M_w) of 365 000) measured using THF as the eluent at 40 °C are significantly higher than the values (M_n = 25 400; M_w = 60 600) obtained at a high temperature of 160 °C using 1,2,4-trichlorobenzene as the eluent (see the Supporting Information). Although PDQT appears soluble in THF at low temperatures, it seems to readily form aggregates composed of several polymer chains, manifesting the strong intermolecular interactions of this polymer. On the other hand, the values obtained at 160 °C using 1,2,4-trichlorobenzene as the eluent should represent the molecular weights of the isolated single polymer chains. A similar chain aggregation phenomenon was observed previously for several other conjugated polymers when their molecular weights were measured using THF as the eluent.[11,12] PDQT displayed absorption maxima, λ_{max}, at 777 and 790 nm in the chloroform solution and in the thin film, respectively (Figure 1). An optical band gap of ∼1.2 eV was calculated from the onset absorption (∼1000 nm) of the polymer thin film. The narrow band gap is indicative of the extensive delocalization of π electrons, which is the result of the extended π-conjugation and the intra- and intermolecular donor (QT)−acceptor (DPP) interactions. The electrochemical properties of PDQT thin films were characterized with cyclic voltammetry (CV) in 0.1 M Bu$_4$NPF$_4$ solution in dry acetonitrile. A reversible oxidation process was observed (Figure 2). The highest occupied molecular orbital (HOMO) energy level of this polymer was calculated from the onset oxidation potential (∼0.8 V) to be 5.2 eV. The reduction process, on the other hand, showed significantly lower currents and was less reversible, indicating that this polymer might favor hole conduction over electron conduction. It is difficult to accurately determine the onset reduction potential from the CV curves. Therefore, the lowest unoccupied molecular orbital (LUMO) energy level of PQT was obtained from the HOMO level (5.2 eV) and the optical band gap (1.2 eV) to be 4.0 eV.

The crystallinity of PDQT was characterized by using differential scanning calorimetry (DSC). During the first heating scan, an exothermic transition temperature at 300 °C was observed, which is attributable to the melting of the polymer backbone (see the Supporting Information). The expected absence of the melting of the side chains indicates that the crystallization of the long, branched 2-octyl-1-dodecyl side chains is prohibited,

Scheme 1. Synthesis of Polymer PDQT[a]

[a] Reagents and conditions: (i) diisopropylsuccinate/t-C_5H_{11}ONa/tert-amyl alcohol/120 °C, 83%; (ii) 2-octyl-1-dodecyl bromide/K_2CO_3/DMF/130 °C, 54%; (iii) Br_2/chloroform/room temperature, 78%; (iv) 5,5′-bis(trimethylstannyl)bithiophene/Pd(PPh$_3$)$_2$Cl$_2$/toluene/90 °C, 99%.

Figure 1. UV–vis–NIR absorption spectra of PDQT and PDQT-a in (a) chloroform solutions and (b) thin films.

Figure 2. Cyclic voltammogram of a PDQT film on a platinum electrode showing the first scan of cathodic and anodic cycles at a scan rate of 100 mV/s in a 0.1 M tetrabutylammonium hexafluorophosphate solution in anhydrous acetonitrile.

while the crystallization of the polymer main chain dominates during the molecular packing. A slightly lower melting point and a smaller enthalpy of transition were observed in the second heating scan. This is likely caused by the partial degradation of the polymer at high temperatures, because the thermogravimetric analysis (TGA) results showed that the decomposition of PDQT starts to occur at ∼350 °C (see the Supporting Information). X-ray diffraction (XRD) analysis of an as-cast, nonannealed PDQT thin film (∼100 nm) on 1-octyltrichlorosilane (OTS)-modified Si/SiO$_2$ substrate further confirmed the crystalline nature of this

polymer, which showed one distinct diffraction peak at $2\theta = 4.4°$, corresponding to a d spacing of 19.9 Å (Figure 3a). Upon thermal annealing at temperatures of 100 and 200 °C, the primary diffraction peak progressively intensified and the second- and third-order peaks became visible. No diffraction originating from the $\pi-\pi$ stacking distance could be observed. This is reminiscent of P3HT[13] and several other polymers[2,5,6,10,14] which form layer-by-layer lamellar structures with the $\pi-\pi$ stacking direction parallel to the substrate in thin films as illustrated in Figure 3b. To further substantiate the edge-on molecular orientation in the polymer thin films, two-dimensional (2-D) transmission XRD measurements were carried out on a stack of polymer thin films with the incident X-ray parallel and perpendicular to the films. As shown in Figure 3c,d, the XRD image and diffractogram obtained with the incident X-ray parallel to the films exhibited diffraction patterns similar to those obtained from the thin film cast on the Si/SiO$_2$ substrate (Figure 3a). On the other hand, data obtained with the incident X-ray perpendicular to the film stack are dramatically different (Figure 3e,f). A strong diffraction peak at $2\theta = 23.7°$ appeared, while the diffraction at $2\theta = 4.4°$ became relatively weak. The peak at $2\theta = 23.7°$ can be assigned to the $\pi-\pi$ stacking distance of ∼3.75 Å. This $\pi-\pi$ stacking distance

Figure 3. XRD intensity graphs of drop-cast PDQT thin films (~100 nm) on OTS-modified Si/SiO$_2$ substrates annealed at different temperatures (a). Illustrative lamellar structures of PDQT in the thin film (b). Respective 2-D XRD image and pattern intensity graph obtained with the incident X-ray parallel to the thin film stack (c, d). Respective 2-D XRD image and pattern intensity graph obtained with the incident X-ray perpendicular to the thin film stack (e, f).

is slightly larger than that (3.71 Å) of PDBT-*co*-TT,[10] indicating the weaker intermolecular interactions of the former, but still relatively small as compared with those (usually 3.8–3.9 Å) of most other conjugated polymers[5,6,15] The above XRD results unambiguously revealed the formation of a highly ordered layer-by-layer lamellar packing motif with an edge-on orientation (Figure 3b) for the annealed and even the nonannealed polymer thin films. This type of molecular organization is particularly favorable for charge carrier hopping through π–π stacks in an OTFT device where the source–drain current flows along the semiconductor layer parallel to the substrate.[13]

PDQT was evaluated as a channel semiconductor in OTFTs using a bottom-gate, top-contact configuration. Heavily doped n$^+$-Si/SiO$_2$ wafer was used as the substrate, wherein the conductive Si wafer and the surface SiO$_2$ layer (~200 nm) function as the common gate electrode and the gate dielectric, respectively. Prior to use, the SiO$_2$ surface was modified with a monolayer of OTS. A PDQT thin film (~35 nm) was deposited

on the substrate by spin-coating a solution of PDQT in chloroform (6 mg/mL) at room temperature and optionally annealed at 100–200 °C on a hot plate under nitrogen in a glovebox. OTFT devices with a channel length (L) of 100 μm and a channel width (W) of 1 mm were then obtained by thermally evaporating gold through a shadow mask to pattern the source and drain electrode pairs. OTFT devices were characterized in a glovebox under nitrogen.

Figure 4 shows the output and transfer curves of two OTFT devices having PDQT thin films without thermal annealing and annealed at 100 °C, respectively. For the OTFT device with the nonannealed thin film, the hole mobility extracted from the saturation regime is 0.89 cm^2/(V·s), with a current on-to-off ratio (I_{on}/I_{off}) of ~10^7 and a threshold voltage (V_T) of −2.6 V. The OTFT device with a PDQT thin film annealed at 100 °C exhibited higher mobility of 0.97 cm^2/(V·s) (I_{on}/I_{off} = ~10^6; V_T = −2.7 V). No further improvements in mobility were observed when the polymer thin films were annealed at a

(a)   (b)

(c)   (d)
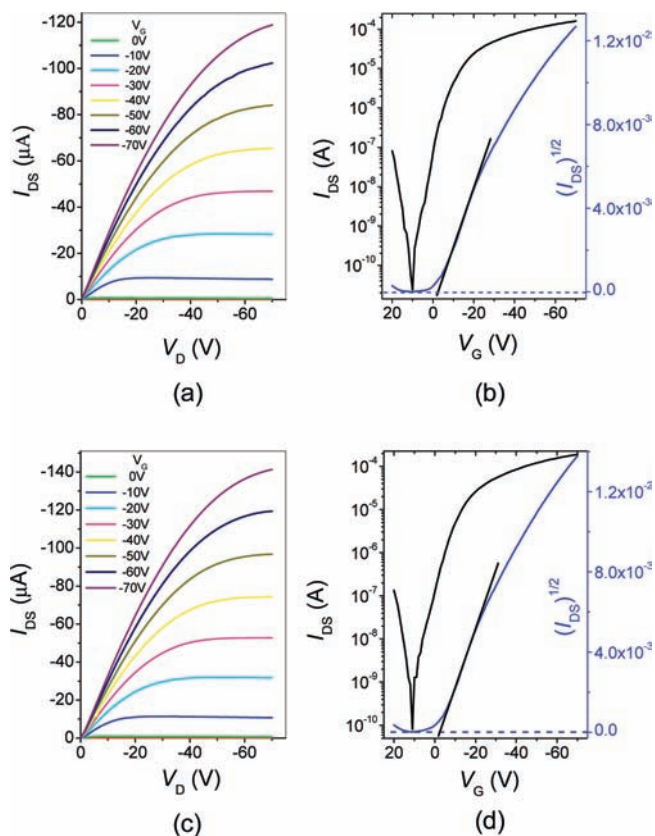
Figure 4. Output (V_G = 0 to -70 V) and transfer ($V_D = -70$ V) characteristics of OTFTs with PDQT thin films without annealing (a, b) and annealed at 100 °C (c, d) (L = 100 μm; W = 1 mm).

temperature beyond 100 °C (up to 200 °C), although the films showed higher crystallinity at higher temperatures (Figure 3a). The fact that PDQT requires a much milder annealing temperature of 100 °C to achieve the maximum mobility as compared with most other high-mobility polymers[2,3,6,7,10,14] indicates that the PDQT polymer chains could readily establish efficient charge transport structures at low temperatures. In our experiments, saturation mobilities of 0.71–0.89 cm^2/(V·s) for nonannealed and 0.80–0.97 cm^2/(V·s) for annealed (100 °C) PDQT thin films were obtained from 12 respective OTFT devices.

The hysteresis characteristics of OTFTs using PDQT were studied by sweeping the gate voltage in both the forward and reverse directions. Figure 5 shows the transfer characteristics of an OTFT with the drain current versus the forward and reverse sweep gate voltages under a source–drain voltage (V_D) of -70 V at a sweep rate of 0.5 V/s. The device hysteresis, which is defined as the difference between the forward and reverse threshold voltages (ΔV_T),[16d] is ~8.0 V. The extent of the hysteresis effect observed for PDQT is similar to that of other common organic semiconductors.[16] The device exhibited hole mobility of 0.91 and 1.06 cm^2/(V·s) in the saturation regime for the forward and the reverse sweeps, respectively.

To investigate the influence of the molecular weight on the mobility, PDQT-a with a lower molecular weight was prepared by shortening the polymerization time. M_n and M_w of PQDT-a were first determined with GPC at 40 °C using THF as the eluent against polystyrene standards to be 45 200 and 97 200, much lower than those (M_n = 106 000; M_w = 365 000) of PQDT measured
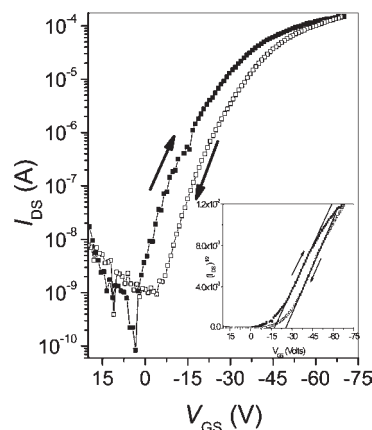

Figure 5. Transfer characteristics of an OTFT using a PDQT thin film annealed at 100 °C with the drain current versus the forward (V_G = +20 to -70 V) and reverse ($V_G = -70$ to +20 V) sweep gate voltages under a V_D of -70 V at a sweep rate of 0.5 V/s. The inset shows the plots of the square root of the drain current versus the gate voltage in forward and reverse sweeps. Arrows indicate the sweeping directions of the gate voltage.

under the same conditions. Surprisingly, M_n and M_w of PDQT-a measured at 160 °C using 1,2,4-trichlorobenzene as the eluent are respectively 21 100 and 50 700, only slightly lower than those of PDQT (M_n = 25 400; M_w = 60 600). The significantly lower molecular weights of PDQT-a measured at 40 °C as compared to those of PDQT suggest that the slightly shorter polymer chains of PDQT-a lead to notably reduced intermolecular interactions. The UV–vis–NIR absorption profiles of PDQT-a in solution and in the solid state are almost identical to those of the high molecular weight PDQT (Figure 1). PDQT-a showed a marginally lower melting temperature (T_m = 298 °C) and a smaller enthalpy of transition (ΔH = 28.7 J/g), as compared with PDQT (T_m = 300 °C; ΔH = 34.1 J/g), suggesting the slightly poorer crystallinity of the former. The XRD patterns of PDQT-a indicate that the polymer chains adopt an edge-on lamellar packing motif similar to that of PDQT (see the Supporting Information). The nonannealed and annealed (at 100 °C) PDQT-a thin films exhibited mobility of 0.35–0.39 cm^2/(V·s) in OTFT devices, substantially lower than the mobility observed for the high molecular weight PDQT.

AFM height images of the nonannealed PDQT thin film show randomly oriented nanorods which further comprise densely packed grains (~20–30 nm) (Figure 6a,d). Upon annealing at 100 °C, the nanorod texture remains similar (Figure 6b), but small holes a few nanometers in diameter appeared on the grains (Figure 6e). On the other hand, the thin film of the low molecular weight PDQT-a shows less defined grains in its AFM images (Figure 6c,f) as compared to that of the high molecular weight PDQT. Furthermore, many pinhole-like voids are observed in the nonannealed PDQT-a thin film, which implies the poor connectivity between grains. Therefore, we believe that the slightly higher molecular weights (or longer chains) of PDQT as compared to PDQT-a could substantially strengthen the intermolecular interactions to form more interconnected crystalline grains, resulting in excellent charge transport performance.[15,17–19]

The exceptionally high hole mobility observed for PDQT can be attributed to a number of factors. First, the enhanced intermolecular interactions arising from (a) the fused aromatic DPP moiety and (b) the donor (QT)–acceptor (DPP) interactions
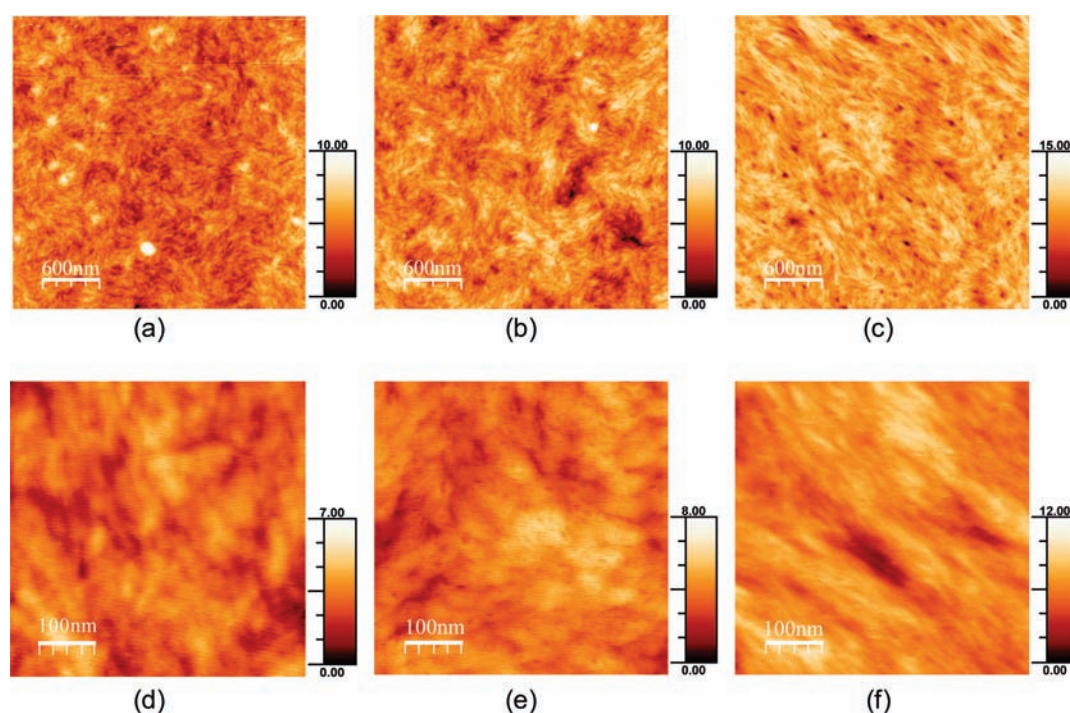
Figure 6. AFM height images of the nonannealed PDQT (a, d), annealed (100 °C) PDQT (b, e), and annealed (100 °C) PDQT-a (c, f) thin films (∼35 nm) on OTS-modified Si/SiO$_2$ substrates.

bring polymer chains into close proximity and form a large $\pi-\pi$ overlap, which facilitate the intermolecular charge hopping through $\pi-\pi$ stacks.[1a,1c] Second, the long electron-donating QT sufficiently compensates the electron-accepting effect of DPP. In comparison to PDQT, other DPP—oligothiophene copolymers with fewer thiophene units such as DPP—bithiophene[9c,9e] and DPP—terthiophene[9d] copolymers (Chart 1) showed considerably lower hole mobility of ≤∼0.1 cm^2/(V·s) and displayed pronounced ambipolar transport characteristics in OTFTs. Third, the use of the β-unsubstituted QT unit provides an adequate spacing to avoid steric interactions between adjacent branched side chains to maintain coplanarity of the polymer backbone. It was reported that a structural analogue of PDQT, poly[3,6-bis(4′-dodecyl[2,2′]bithiophenyl-5-yl)-2,5-bis(2-hexyldecyl)-2,5-dihydropyrrolo[3,4-*c*]pyrrole-1,4-dione], which has side chain substitution on the inner bithiophene moiety, exhibited much lower mobility (∼0.1 cm^2/(V·s)).[9a] The crowded side chain substitution in this polymer might perturb the main chain coplanarization and the intermolecular interactions in the solid state, resulting in less ordered molecular organization. Finally, the sufficiently high molecular weight of PDQT enables the polymer chains to self-assemble into densely packed nanometer-sized grains through intensified intermolecular interactions, which interconnect the crystalline grains to provide efficient pathways for intergranular charge transport.[15,17−19] The slightly weakened intermolecular interactions as compared with PDBT-*co*-TT[10] allow the spontaneous formation of well-interconnected thin film morphology with a highly ordered, crystalline structure after solution deposition without a subsequent high-temperature treatment, which accounts for the high mobility achieved for the nonannealed PDQT thin films.

■ CONCLUSIONS

A donor—acceptor DPP—quaterthiophene copolymer PDQT was designed and synthesized. Substitution of the DPP unit with a long, branched 2-octyl-1-dodecyl side chain afforded excellent solubility of PDQT in various solvents. Thermal analysis and XRD results suggested that PDQT is highly crystalline and could readily form crystalline thin films with preferential edge-on molecular orientation after solution deposition even without thermal annealing. It was found that the molecular weight of the polymer significantly influences the thin film morphology. The high polymer weight PDQT formed thin films comprising densely packed nanometer-sized grains, while the thin film of the low molecular weight PDQT-a formed poorly interconnected structures with populous pinholes. The high molecular weight PDQT showed high hole mobility of up to 0.89 cm^2/(V·s) in OTFTs with spin-coated PDQT thin films without thermal annealing, which is close to the maximum mobility of ∼0.97 cm^2/(V·s) achieved for polymer thin films annealed at 100 °C. On the other hand, the low molecular weight PDQT-a exhibited substantially lower mobility of 0.35−0.39 cm^2/(V·s) under similar fabrication conditions. The significantly high hole mobility observed for PDQT processed at mild temperatures might be contributable to (i) the strong intermolecular interactions arising from the fused ring DPP moiety and the intermolecular donor—acceptor interaction that facilitate charge hopping through $\pi-\pi$ stacks, (ii) the pronounced hole transport capability by using a sufficiently long electron-donating quaterthiophene, (iii) the spaced out side chain arrangement by using β-unsubstituted quaterthiophene to help polymer chains self-assemble into highly ordered crystalline structures, and (iv) the sufficiently high molecular weight that enables polymer chains to form well-interconnected crystalline grains to establish efficient pathways for intergranular charge transport. The high mobility, not requiring annealing, excellent solution processability, and facile synthesis have rendered this polymer potentially useful for high-throughput, roll-to-roll manufacturing of low-cost OTFT circuits and arrays for a wide range of electronic applications.

■ ASSOCIATED CONTENT

ⓈSupporting Information.   Experimental details and additional graphs. This material is available free of charge via the Internet at http://pubs.acs.org.

■ AUTHOR INFORMATION

Corresponding Author
yuning.li@uwaterloo.ca

■ ACKNOWLEDGMENT

■ REFERENCES

(1) (a) Horowitz, G. *Adv. Mater.* **1998**, *10*, 365. (b) Sirringhaus, H.; Tessler, N.; Friend, R. H. *Science* **1998**, *280*, 1741. (c) Dimitrakopoulos, C. D.; Malenfant, P. R. L. *Adv. Mater.* **2002**, *14*, 99. (d) Katz, H. E. *Chem. Mater.* **2004**, *16*, 4748. (e) Allard, S.; Forster, M.; Souharce, B.; Thiem, H.; Scherf, U. *Angew. Chem., Int. Ed.* **2008**, *47*, 2. (f) Ong, B. S.; Wu, Y.; Li, Y.; Liu, P.; Pan, H. *Chem.—Eur. J.* **2008**, *14*, 4766. (g) Sirringhaus, H.; Bird, M.; Richards, T.; Zhao, N. *Adv. Mater.* **2010**, *22*, 3812.

(2) McCulloch, I.; Heeney, M.; Bailey, C.; Genevicius, K.; Macdonald, I.; Shkunov, M.; Sparrowe, D.; Tierney, S.; Wagner, R.; Zhang, W. M.; Chabinyc, M. L.; Kline, R. J.; McGehee, M. D.; Toney, M. F. *Nat. Mater.* **2006**, *5*, 328.

(3) Tsao, H. N.; Cho, D.; Andreasen, J. W.; Rouhanipour, A.; Breiby, D. W.; Pisula, W.; Müllen, K. *Adv. Mater.* **2009**, *21*, 209.

(4) (a) MacDonald, W. A. *J. Mater. Chem.* **2004**, *14*, 4. (b) Klauk, H., Ed. *Organic Electronics: Materials, Manufacturing and Applications*; Wiley-VCH Verlag GmbH & Co. KGaA: Weinheim, Germany, 2006; Chapter 7.

(5) Pan, H.; Li, Y.; Wu, Y.; Liu, P.; Ong, B. S.; Zhu, S.; Xu, G. *J. Am. Chem. Soc.* **2007**, *129*, 4112.

(6) Li, Y.; Wu, Y.; Liu, P.; Birau, M.; Pan, H.; Ong, B. S. *Adv. Mater.* **2006**, *18*, 3029.

(7) Osaka, I.; Sauvé, G.; Zhang, R.; Kowalewski, T.; McCullough, R. D. *Adv. Mater.* **2007**, *19*, 4160.

(8) Kong, H.; Jung, Y. K.; Cho, N. S.; Kang, I.-N.; Park, J.-H.; Cho, S.; Shim, H.-K. *Chem. Mater.* **2009**, *21*, 2650.

(9) (a) Bürgi, L.; Turbiez, M.; Pfeiffer, R.; Bienewald, F.; Kirner, H.; Winnewisser, C. *Adv. Mater.* **2008**, *20*, 2217. (b) Turbiez, M.; Janssen, R.; Wienk, M.; Kirner, H.; Düggeli, M.; Tieke, B.; Zhu, Y. W.O. Patent Application 2008/00064 A1, 2008. (c) Li, Y. U.S. Patent Application 2009/65766 A1, 2009. (d) Bijleveld, J. C.; Zoombelt, A. P.; Mathijssen, S. G. J.; Wienk, M. M.; Turbiez, M.; de Leeuw, D. M.; Janssen, R. A. J. *J. Am. Chem. Soc.* **2009**, *131*, 16616. (e) Zoombelt, A. P.; Mathijssen, S. G. J.; Turbiez, M. G. R.; Wienk, M. M.; Janssen, R. A. J. *J. Mater. Chem.* **2010**, *20*, 2240.

(10) Li, Y.; Singh, S. P.; Sonar, P. *Adv. Mater.* **2010**, *22*, 4862.

(11) Li, Y.; Vamvounis, G.; Holdcroft, S. *Chem. Mater.* **2002**, *14*, 1424.

(12) Zhou, H.; Yang, L.; Liu, S.; You, W. *Macromolecules* **2010**, *43*, 10390.

(13) Sirringhaus, H.; Brown, P. J.; Friend, R. H.; Nielen, M. M.; Bechgaard, K.; Langeveld-Voss, B. M. W.; Spiering, A. J. H.; Janssen, R. A. J.; Meijer, E. W.; Herwig, P.; de Leeuw, D. M. *Nature* **1999**, *401*, 685.

(14) Ong, B. S.; Wu, Y.; Liu, P.; Gardner, S. *J. Am. Chem. Soc.* **2004**, *126*, 3378.

(15) Kline, R. J.; McGehee, M. D.; Kadnikova, E. N.; Liu, J.; Fréchet, J. M. J.; Toney, M. F. *Macromolecules* **2005**, *38*, 3312.

(16) (a) Gu, G.; Kane, M. G.; Doty, J. E.; Firester, A. H. *Appl. Phys. Lett.* **2005**, *87*, 243512. (b) Lee, C. A.; Park, D. W.; Jin, S. H.; Park, I. H.;

Lee, J. D.; Park, B. G. *Appl. Phys. Lett.* **2006**, *88*, 252102. (c) Veres, J.; Ogier, S. D.; Leeming, S. W.; Cupertino, D. C.; Khaffaf, S. M. *Adv. Funct. Mater.* **2003**, *13*, 199. (d) Yang, N. J.; Liao, C. S.; Chen, S. A. *Adv. Funct. Mater.* **2010**, *20*, 1000.

(17) Verilhaca, J.-M.; LeBlevennec, G.; Djurado, D.; Rieutord, F.; Chouiki, M.; Travers, J.-P.; Pron, A. *Synth. Met.* **2006**, *156*, 815.

(18) Chang, J.-F.; Clark, J.; Zhao, N.; Sirringhaus, H.; Breiby, D. W.; Andreasen, J. W.; Nielsen, M. M.; Giles, M.; Heeney, M.; McCulloch, I. *Phys. Rev. B* **2006**, *74*, 115318.

(19) Singh, K. A.; Sauvé, G.; Zhang, R.; Kowalewski, T.; McCullough, R. D.; Porter, L. M. *Appl. Phys. Lett.* **2008**, *92*, 263303.